Extrasynaptic CaMKIIα is involved in the antidepressant effects of ketamine by downregulating GluN2B receptors in an LPS-induced depression model

Xiao-Hui Tang
southeast university
Guang-Fen Zhang
southeast university
Ning Xu
Southeast University Zhongda Hospital
Gui-Fang Duan
nanjing university
Min Jia
nanjing university
Ru Liu
nanjing university
Zhi-Qiang Zhou
Jinling hospital
Jian-Jun Yang (yjyangjj@126.com)
the first hospital of zhengzhou university

Research

Keywords: Ketamine, Extrasynaptic, CaMKIIα, GluN2B, Depression

Posted Date: February 8th, 2020

DOI: https://doi.org/10.21203/rs.2.22906/v1

Version of Record: A version of this preprint was published at Journal of Neuroinflammation on June 10th, 2020. See the published version at https://doi.org/10.1186/s12974-020-01843-z.

Abstract

Background A subanesthetic dose of ketamine provides rapid and effective antidepressant effects, but the molecular mechanism of this treatment remains elusive. Methods In this study, we investigated the role of CaMKIIα in the antidepressant effects of ketamine using an LPS-induced mouse model of depression, explored the different changes of CaMKIIα in the synaptic and extrasynaptic regions of the hippocampus, and clarified the relationship between CaMKIIα and GluN2B from extrasynaptic perspective. Results Ketamine (10 mg/kg, i.p.) administration attenuated the LPS-induced increase in extrasynaptic CaMKIIα activity (p-CaMKIIα) and extrasynaptic GluN2B localization and phosphorylation and that ketamine exerted antidepressant effects. Immunoprecipitation assay revealed that in the extrasynaptic region of the hippocampus, p-CaMKIIα bound to GluN2B, and ketamine administration attenuated the enhanced interaction between p-CaMKIIα and GluN2B induced by LPS. KN93, a CaMKIIα inhibitor, could also reverse the high level of extrasynaptic p-CaMKIIα, reduce hippocampal extrasynaptic GluN2B localization and phosphorylation, and exert antidepressant effects. Additional changes downstream of the ketamine-induced changes in extrasynaptic GluN2B included rescuing the downregulated expression of p-CREB, BDNF, and GluR1 and reversing the impaired induction of LTP in the hippocampus induced by LPS. Conclusion These results indicate that extrasynaptic CaMKIIα plays a key role in the cellular mechanism of ketamine's antidepressant effect and is related to the down-regulation of extrasynaptic GluN2B localization and phosphorylation and further affects synaptic plasticity.

Background

Depression is a common clinical psychiatric disease, and epidemiology shows that it affects about 16% of the global population, creating a serious social burden [1]. However, traditional antidepressants often require several weeks or months of continuous medication to achieve a better therapeutic effect [2]. Therefore, it is urgent to find a new type of antidepressant that can work quickly. A single low dose of ketamine has a rapid and effective antidepressant effect, which has been confirmed by many laboratories [3–5]. Although there have been many preclinical studies that have shown us the possible direction of ketamine's antidepressant mechanism, its exact molecular mechanism is unclear.

Calcium/calmodulin-dependent protein kinase II (CaMKII) is a Ser/Thr protein kinase widely distributed in the brain, which is encoded by four genes α, β, γ and δ. In the hippocampus, CaMKIIα is the most abundant subtype, occupying a critical position in the transmission of synaptic signals and the regulation of synaptic morphology [6–8]. Stress-induced activation of hypocretin/orexin receptors produces depression-like behaviors through an increase in p-CaMKIIα in mice and that siRNA-mediated inhibition of CaMKIIα rescues the depressive-like behaviors [9]. In addition, Fluoxetine, a typical antidepressant, reduces the binding of the transcription factor ΔfosB to the promoter of CaMKIIα, thereby reducing the expression of CaMKII. Similarly, inhibition of CaMKII reverses depression-like behaviors, whereas overexpression of CaMKII occludes fluoxetine’s antidepressant actions [10]. The above studies indicated that in the emergence of stress-induced depression-like behaviors and the therapeutic effects of

traditional antidepressants, CaMKIIα occupies a critical position, but whether CaMKIIα was involved in ketamine's rapid antidepressant action remains unclear.

N-methyl-D-aspartate receptors (NMDARs) NMDAR is the most common type of ionotropic glutamate receptors in the brain. Most functional NMDA receptors are tetramers formed by the GluN1 subunit and multiple GluN2 subunits. Because of the different localization of NMDARs on the synapse, they can be further divided into synaptic NMDARs and extrasynaptic NMDARs. Among them, the studies of extrasynaptic NMDARs have shown that it contains the GluN2B subunit [11, 12]. It has been confirmed that knocking out the GluN2B subunit in principal cortical neurons of the mouse occludes ketamine's antidepressant actions [13]. Meanwhile, GluN2B-selective antagonists were observed to have antidepressant effects in various animal models of depression [14–16] and the NMDAR antagonists that preferentially bind to GluN2B can effectively improve the clinical symptoms of depressed patients [17]. The above results suggest that the GluN2B subunit is closely related to the antidepressant effect of ketamine and the improvement of depressive symptoms, but the upstream and downstream involved in GluN2B involvement in this process remains unclear.

Under physiological conditions, when intracellular calcium ions are in a steady state, CaMKIIα is in an inactive state, and CaMKIIα is activated when calcium ions enter the cells via various ion channels. The activation of CaMKIIα ultimately promotes autophosphorylation at threonine 286 (p-CaMKIIα), which binds to GluN2B and phosphorylates GluN2B at the S1303 site (p-GluN2B) [18–20]. The synaptic binding of CaMKIIα/GluN2B has been intensively studied [21–23]. Studies have shown that the interaction between GluN2B and CaMKIIα is important for synaptic CaMKIIα localization and activity [19, 24]. In addition, CaMKIIα occupies an important position in the regulation of a series of physiological processes, including the regulation of synaptic plasticity, which is a key component of the efficacy of antidepressants [25]. However, it remains unclear whether the extrasynaptic CaMKIIα/GluN2B is involved and how it is involved in the antidepressant process of ketamine. Hence, in this study, we investigated the changes in extrasynaptic CaMKIIα and GluN2B, as well as the interaction between CaMKIIα and GluN2B, in the antidepressant effects of ketamine using a lipopolysaccharide (LPS)-induced depression model. Furthermore, we examined the downstream molecules impacted by GluN2B that may be involved in ketamine's antidepressant effects.

Materials And Methods

Animals

Male adult C57BL/6J mice (25–30 g) obtained from the Model Animal Research Center (MARC) of Nanjing University, Nanjing, China. Four-five individuals were placed in each cage, and the mice were maintained in a room temperature of 23 ± 1 ℃, with a 12 h light/dark cycle. The mice were free to food and water. All animal experiments and related operations are carried out in accordance with the Guideline for the Care and Use of Laboratory Animals from the National Institutes of Health, USA. The mice were acclimated to the environment and individually handled every day for 7 days before the experiments.

Lps-induced Depression Model

The LPS-induced depression model was based on previous studies but with some changes [26]. In this experiment, the injection dose of LPS (1 mg/kg, i.p.) was selected based on previous studies [27]. LPS dissolved in physiological saline and then injected at a volume of 1 ml/kg in all conditions. The solution is ready for use and the intraperitoneal injection of LPS was scheduled at a fixed time (09:00 and 10:00 a.m).

Experimental Design And Drug Administration

Experiment 1: mice were randomly numbered and then divided into 4 groups: the Sal + Sal group; the LPS + Sal group; the Sal + Ket group; and the LPS + Ket group. First, LPS (1 mg/kg) or physiological saline (equal volume) was injected intraperitoneally between 09:00 and 10:00 a.m. After 23.5 hours, ketamine (10 mg/kg) or physiological saline (equal volume) was injected intraperitoneally. The open field test (OFT), novelty-suppressed feeding test (NSFT) and forced swim test (FST) were performed 0.5 h after ketamine administration. In each group of mice, half performed behavioral tests and the other half carried out biochemical tests. The flow chart of Experiment 1 is shown in Fig. 1a.

Experiment 2: mice were randomly numbered and then divided into 4 groups: the Sal + dimethyl sulfoxide (DMSO) group; the LPS + DMSO group; the Sal + KN-93 group; and the LPS + KN-93 group. First, LPS (1 mg/kg) or physiological saline (equal volume) was injected intraperitoneally between 09:00 and 10:00 a.m. After 23.5 hours, KN-93 (10 mg/kg) or DMSO (equal volume) was injected intraperitoneally. The dose selection of KN93 in this experiment is based on the pre-experiment results. The NSFT and FST were performed 0.5 h after KN-93 administration. In each group of mice, half performed behavioral tests and the other half carried out biochemical tests. The flow chart of Experiment 2 is shown in Fig. 1b.

Both ketamine hydrochloride (Gutian Pharmaceutical Company, China) and LPS (L-2880, Sigma, USA) were dissolved in physiological saline. KN-93 (S7423, Selleckchem, USA) was dissolved in 1% DMSO. In this study, the intraperitoneal injection volume of all drugs was based on 7.5 ml/kg body weight.

Behavioral Tests

Behavioral experiments are carried out in quiet rooms using an XR-XZ301 instrument (Xinruan Corporation, Shanghai, China). All behavioral data were analyzed by a researcher blinded to the experimental grouping.

Open Field Test

Mice were placed in a white experimental box (40 cm × 40 cm × 40 cm; length × width × height) and allowed to move freely for 5 minutes. The entire process was automatically tracked by a camera placed

above the experimental box. The total distance traveled was considered to be a measure of the ability of the mouse to move. The central area residence time and number of visits were considered to be a measure of the level of anxiety in mice. At the end of each test, wipe the instrument with 75% alcohol to avoid the effect of the residual odor of the previous animal on the test results.

Novelty-suppressed Feeding Test

The mice were fasted 12 hours before the experiment and the drinking water was not limited [28]. Before the experiment, two pieces of chow were placed in the center of a plastic box (40 × 40 × 40 cm). Then, mice were placed in the test box and allowed to move freely for 10 minutes. The time required for the mouse to enter the box to eat food for the first time is the feeding latency. The feeding latency was considered to be a measure of the level of depression in mice. At the end of the experiment, mice were placed in a cage with pre-weighed food, and the consumption of this food was recorded for 15 minutes.

Forced Swimming Test

Mice were placed in a glass container (18 cm diameter × 28 cm height) of water (15 cm; 25 ± 1 ℃) and allowed to swim under normal light for 6 minutes and recorded the total immobility time of the last 4 minutes [29]. The definition of immobility time refers to the time when the mouse passively floated with no additional activity or with no other movements except those to maintain balance in the water. After the experiment, the mouse body was wiped dry with absorbent paper and placed back in the original cage. Replace the water at the end of each test.

Western Blot Analysis

Tissue preparation and subcellular fractionation

The levels of p-CaMKIIα, CaMKIIα, p-GluN2B and GluN2B in the synaptic and extrasynaptic fractions of the hippocampus were assessed by Western blotting. The separation methods of the synaptic and extrasynaptic fractions refer to previous studies [30]. Briefly, the hippocampus of adult mice was dissected and homogenized in an ice-cold sucrose buffer (in mM): 320 sucrose, 10 Tris (pH 7.4), 1 EDTA, 1 Na_3VO_4, 5 NaF, 1 EGTA and 1X protease inhibitor cocktail, and then centrifuged at 1,000 g for 10 minutes at 4 °C. The supernatant (S1) was collected and centrifuged at 10,000 g for 20 minutes at 4 °C. Then, the pellet (P2) was saved and resuspended in sucrose buffer. Then, the pellet (P2) was centrifuged at 10,000 g for 20 minutes at 4 °C and repeated twice. Then, the pellet (P2) was resuspended in an ice-cold Triton X-100 buffer (in mM): 10 Tris (pH 7.4), 1 EDTA, 1 Na_3VO_4, 5 NaF, 1 EGTA and 0.5% Triton X-100. This pellet (P2) was rotated slowly20 min at 4 °C. Then, the pellet (P2) was centrifuged at 32,000 g for 20 minutes at 4 °C. The supernatant and pellet comprised the extrasynaptic fraction (Non-PSD) and synaptic fraction (PSD), respectively. The separation of the synaptic and extrasynaptic fraction was

demonstrated by the distribution of postsynaptic density-95 (PSD95) and synaptophysin. The protein concentration of the four groups were measured by bicinchoninic acid (BCA) protein assay and then adjusted to the same level.

Total Protein Preparation

The levels of p-CREB, CREB and BDNF in the total protein of hippocampus were assessed by Western blotting. Briefly, the hippocampus of adult mice was harvested on the ice and then homogenized in an ice-cold protein lysis buffer (in mM): 150 NaCl, 50 Tris-HCl, 0.1% SDS, 1% Triton X-100, 1% sodium deoxycholate, 1 NaF, 1 Na_3VO_4, 1 PMSF, and 1X protease inhibitor cocktail. The homogenate was centrifuged at 10,000 rpm for 10 minutes at 4 °C. Then, the protein concentration of the four groups were measured by BCA protein assay and then adjusted to the same level.

Synaptosome Preparation

The levels of GluR1 and GluR2 in the synaptosome of hippocampus were assessed by Western blotting. The separation methods of the synaptosome fractions refer to previous studies[31]. Briefly, the hippocampus of adult mice was harvested on the ice and then homogenized in an ice-cold sucrose solution (in mM): 320 sucrose, 20 HEPES (pH 7.4), 1 Na3VO4, 1 EDTA, 5 NaF, and 1X protease inhibitor cocktail, and then centrifuged at 28,00 rpm for 10 minutes at 4 °C. The supernatant was collected and centrifuged at 12,000 rpm for 10 minutes at 4 °C. Then, the pellet (synaptosome fraction) was saved and resuspended in an ice-cold protein lysis buffer (in mM): 150 NaCl, 50 Tris-HCl (pH 7.4), 1% Triton X-100, 0.1% SDS, 1 Na3VO4, 2 EDTA, 5 NaF, and 1X protease inhibitor cocktail. The protein concentration of the four groups were measured by BCA protein assay and then adjusted to the same level.

Protein (10–20 μg/well) were separated by 8–12% SDS-PAGE gels and then transferred to polyvinylidene fluoride membranes. 5% non-fat milk was used to incubate the membranes for 2 h at room temperature. After this, the membranes were incubated primary antibody overnight at 4 °C. The selected primary antibody is as follows: anti-BDNF (Abcam, Cambridge, UK); anti-CaMKIIα (phospho-T286) (Abcam, Cambridge, UK); anti-CaMKIIα (Abcam, Cambridge, UK); anti-CREB (Cell Signaling, MA, USA); anti-GAPDH (ProteinTech, USA); anti-β-actin (GeneTex, USA); anti-PSD95 (Millipore, MA, USA); anti-Synaptophysin (Millipore, MA, USA); anti-NMDAR2B (phospho-S1303) (Abcam, Cambridge, UK); anti-Glutamate Receptor 1 (Abcam, Cambridge, UK); anti-NMDAR2B (Abcam, Cambridge, UK); anti-CaMKIIβ (Abcam, Cambridge, UK); anti-p-CREB (Cell Signaling, MA, USA) and anti-Glutamate Receptor 2 (Abcam, Cambridge, UK). The membranes were washed three times in TBST and then incubated in the corresponding secondary antibody (goat anti-rabbit or mouse and rabbit anti-goat; Bioworld Technology, MN, USA) for 2 h at room temperature. Finally, the protein bands were visualized by chemiluminescence method. The mean gray value of each protein band was quantified by ImageJ (NIH, Bethesda, MD, USA).

Immunofluorescence

Mice were anesthetized with 1% sodium pentobarbital (50 mg/kg, i.p.; Sigma, USA), followed by systemic perfusion of the mice via the left ventricle using physiological saline and 4% PFA. Then, the whole brain of the mice was taken out and dipped in 4% PFA for 4–6 hours at 4 °C. After that, the brain was dehydrated in 20% and 30% sucrose at 4 °C, respectively. OCT was used to embed the brain when it sinks to the bottom. A 10 μm thick coronal sections of hippocampus were cut and immediately adhered to the slide. The slides were immersed in the PBS for 10 minutes to wash away the OCT during embedding. Next, the slides were blocked with 10% goat serum for 2 h at room temperature. After that, slides were incubated in primary antibodies diluted with 5% BSA overnight at 4 ℃: anti-NMDAR2B (phospho-S1303) (Abcam, Cambridge, UK); anti-NMDAR2B (Abcam, Cambridge, UK); and anti-PSD95 (Millipore, MA, USA). The slides were washed with PBS (with 5‰ Triton X-100) for 3 × 5 min. Then, the slides were incubated in corresponding secondary antibodies (Alexa Fluor 488/549 goat anti-rabbit or mouse; Bioworld Technology, MN, USA) for 2 h at room temperature. After washing with PBS (with 5‰ Triton X-100) for 3 × 5 min, the slides were incubated with DAPI to label nuclei. A confocal scanning microscope (Carl Zeiss, LSM880, Germany) was used to obtain the fluorescence images of the region of interest. The Pearson's coefficient colocalization was used to quantify the colocalization of two confocal immunofluorescences, which was calculated by a plug-in package in ImageJ (NIH, Bethesda, MD, USA).

Immunoprecipitation

Immunoprecipitation was used to detect the interaction between p-CaMKIIα and GluN2B. Immunoprecipitation from the extrasynaptic fractions of the hippocampus was performed with rabbit NMDAR2B (2–3 μg) antibody [32]. Briefly, the extrasynaptic fractions of the hippocampus were obtained as described above. The extracts were precleared by adding nonspecific control immunoglobulin G (1 μg) and 20 μl of Protein G Sepharose (Sigma, USA). The supernatant was collected and incubated with nonspecific IgG (2 μg) or rabbit anti-NMDAR2B (2 μg; Abcam, Cambridge, UK) overnight at 4 ℃. The next day, they were mixed with the addition of 40 μl of Protein G Sepharose (Sigma, USA) and then rotated slowly for 4 hours at 4 °C. After that, the beads were washed three times in Buffer A (in mM): 150 NaCl, 50 Tris-HCl, 0.1% Triton X-100, and 1 EDTA. Then, the beads were washed three times in Buffer B (in mM): 300 NaCl, 50 Tris-HCl, 0.1% Triton X-100, and 1 EDTA. Finally, the beads were denatured in SDS buffer and separated by SDS-PAGE.

Electrophysiological Recording

The mice were anesthetized and the whole brain was taken out on the ice. The brain was quickly dipped in a pre-oxygenated (95% O_2/5% CO_2) cutting solution (in mM): 2.6 KCl, 1.25 NaH_2PO_4, 26 $NaHCO_3$, 0.5 $CaCl_2$, 5 $MgCl_2$, 212 sucrose and 10 dextrose for 2 minutes. In the cutting solution, a 300 μm thick coronal slices of hippocampus were cut out. Then, the slices were immediately transferred to the artificial

cerebrospinal fluid (ACSF) (in mM): 124 NaCl, 5 KCl, 1.25 NaH_2PO_4, 26 $NaHCO_3$, 2 $CaCl_2$, 2 $MgCl_2$, and 10 dextrose for incubation. The hippocampal slices were then kept at 26 °C for 1 hour before recording. In order to induce LTP, concentric bipolar tungsten electrodes and the recording pipettes were placed in the Schaffer collateral–commissural fibers and the stratum radiatum of hippocampal CA1 region, respectively. During the recording period, ACSF was perfused continuously and the Picrotoxin (0.1 mM) and APV (80 μM) were added to the ASCF to block $GABA_A$ and NMDA receptors, respectively. In this study, LTP was evoked by high-frequency stimulation (HFS; three trains of 100 Hz with a 10 s interval between each train). A steady baseline was recorded for at least 10 minutes before the induction of LTP. The field excitatory postsynaptic potential (fEPSP) slope between 10% and 90% was used to indicate the fEPSP magnitude. Data are normalized to the mean baseline value and shown as mean ± S.E.M. Slices were considered to demonstrate LTP if the amplitude of the fEPSP were increased by at least 15% compared to baseline. The signal was amplified with pClamp 700B amplifier (Axon Instruments, Foster City, CA), acquired at 10 kHz and filtered at 2 kHz.

Statistical analysis

Data are shown as mean ± SEM. SPSS software (version 25.0, IL, USA) and GraphPad Prism (version 7, CA, USA) were used for statistical analyses. Shapiro-Wilk test and Levene's test were used for the distribution and variance analysis of the data. When data were not normally distribution, the differences among groups was detected by Kruskal–Wallis one-way ANOVA followed by Bonferroni's correction. When data were normally distributed, the differences among groups was detected by two-way ANOVA followed by Bonferroni's multiple comparisons test. LPS injection and ketamine or KN93 administration were considered two independent factors. $P < 0.05$ indicates that the difference is statistically significant.

Results

Ketamine improved LPS-induced depression-like behaviors

No significant difference in the total travelled distance within 5 minutes was observed in the four groups, indicating that LPS injection and ketamine administration do not affect the locomotor activity of mice (Fig. 2a; interaction: LPS × ketamine, $F_{1,24} = 2.54$, $P > 0.05$; LPS: $F_{1,24} = 3.735$, $P > 0.05$; ketamine: $F_{1,24} = 3.663$, $P > 0.05$; LPS is LPS + Sal versus Sal + Sal; ketamine is LPS + Ket versus LPS + Sal). LPS injection decreased the time spent in the center (interaction: LPS × ketamine, $F_{1,24} = 4.40$, $P < 0.05$; LPS: $F_{1,24} = 8.869$, $P < 0.01$; ketamine: $F_{1,24} = 20.273$, $P < 0.01$) and the number of entries into the center (interaction: LPS × ketamine; $F_{1,24} = 18.253$, $P < 0.05$; LPS: $F_{1,24} = 5.116$, $P < 0.05$; ketamine: $F_{1,24} = 18.253$, $P < 0.01$), both of these effects were rapidly reversed by ketamine administration (Fig. 2b). Ketamine treatment reversed the LPS-induced increase in the feeding latency (interaction: LPS × ketamine, $F_{1,24} = 21.226$, $P < 0.05$; LPS: $F_{1,24} = 30.552$, $P < 0.01$; ketamine: $F_{1,24} = 30.165$, $P < 0.01$) of the NSFT; however, the total food consumption (interaction: LPS × ketamine, $F_{1,24} = 1.126$, $P > 0.05$; LPS: $F_{1,24} = 4.504$, $P > 0.05$; ketamine: $F_{1,24} = 0.681$, $P > 0.05$) in the home cage in a 15-min test of the four groups was not affected (Fig. 2c). In

the FST, LPS increased the immobility time (interaction: LPS × ketamine, $F_{1,24} = 15.13$, $P < 0.05$; LPS: $F_{1,24} = 13.414$, $P < 0.01$; ketamine: F1,24 = 22.327, $P < 0.01$), which reversed by ketamine treatment (Fig. 2d). In summary, these behavioral results indicated that ketamine (10 mg/kg) administration can eliminate the depression and anxious-like behaviors caused by LPS injection without affecting the locomotor activity of mice.

Ketamine Reversed Lps-induced Extrasynaptic Camkiiα Activity In The Hippocampus

The expression of p-CaMKIIα (T286) was used to indicate the activity of CaMKIIα. In the extrasynaptic fractions of the hippocampus, ketamine administration reversed the elevated level of p-CaMKIIα induced by LPS injection (Fig. 3a; interaction: LPS × ketamine, $F_{1,12} = 11.495$, $P < 0.05$; LPS: $F_{1,12} = 5.710$, $P < 0.05$; ketamine: $F_{1,12} = 5.604$, $P < 0.05$). In contrast, no significant difference in the level of p-CaMKIIα was observed in the four groups (Fig. 3b; interaction: LPS × ketamine, $F_{1,12} = 0.426$, $P > 0.05$; LPS: $F_{1,12} = 0.000$, $P > 0.05$; ketamine: $F_{1,12} = 0.015$, $P > 0.05$).

Ketamine reversed the LPS-mediated extrasynaptic GluN2B localization and phosphorylation in the hippocampus

In the extrasynaptic fractions, ketamine treatment reversed the LPS-induced increase in the level of GluN2B (Fig. 4a; interaction: LPS × ketamine, $F_{1,12} = 3.267$, $P > 0.05$; LPS: $F_{1,12} = 7.045$, $P < 0.05$; ketamine: $F_{1,12} = 5.224$, $P < 0.05$). However, in the synaptic fractions, no significant difference in the level of GluN2B was observed in the four groups (Fig. 4a; interaction: LPS × ketamine, $F_{1,12} = 0.172$, $P > 0.05$; LPS: $F_{1,12} = 0.020$, $P > 0.05$; ketamine: $F_{1,12} = 0.775$, $P > 0.05$). Next, to confirm this finding, dual antibody labeling of surface GluN2B (an antibody that specifically binds to the N-terminal of the GluN2B) and synapse-specific protein PSD95 were used to identify synaptic GluN2B localization. Pearson's correlation coefficient was used to indicate the overlap and correlation of fluorescent intensity in the two different labels. In the CA1, CA3 and DG of hippocampus, no significant difference in the colocalization of GluN2B and PSD95 was observed in the four groups (Fig. 4e; CA1: interaction: LPS × ketamine, $F_{1,20} = 0.109$, $P > 0.05$; LPS: $F_{1,20} = 0.981$, $P > 0.05$; ketamine: $F_{1,20} = 0.303$, $P > 0.05$; CA3: interaction: LPS × ketamine, $F_{1,20} = 2.381$, $P > 0.05$; LPS: $F_{1,20} = 0.000$, $P > 0.05$; ketamine: $F_{1,20} = 0.381$, $P > 0.05$; DG: interaction: LPS × ketamine, $F_{1,20} = 0.000$, $P > 0.05$; LPS: $F_{1,20} = 0.155$, $P > 0.05$; ketamine: $F_{1,20} = 0.843$, $P > 0.05$). This result suggests that ketamine did not affect synaptic GluN2B localization. In the CA1 and DG of hippocampus, ketamine administration reversed the LPS-induced increase in the expression of GluN2B (Fig. 4f; CA1: interaction: LPS × ketamine, $F_{1,12} = 17.929$, $P < 0.05$; LPS: $F_{1,12} = 16.714$, $P < 0.01$; ketamine: $F_{1,12} = 14.044$, $P < 0.01$; DG: interaction: LPS × ketamine, $F_{1,12} = 33.842$, $P < 0.05$; LPS: $F_{1,12} = 52.299$, $P < 0.01$; ketamine: $F_{1,20} = 30.386$, $P < 0.01$). Combined with the above results and given that ketamine

administration did not affect synaptic GluN2B localization, this result suggests that the ketamine-mediated reduction in GluN2B mainly affects extrasynaptic sites. Furthermore, in the extrasynaptic fractions, ketamine treatment reversed the LPS-induced increase in the level of p-GluN2B (S1303) (Fig. 4b; LPS: H = 8.824, P < 0.05; ketamine: H = 8.824, P < 0.05). However, in the synaptic fractions, no significant difference in the level of p-GluN2B was observed in the four groups (Fig. 4b; interaction: LPS × ketamine, $F_{1,12}$ = 0. 144, P > 0.05; LPS: $F_{1,12}$ = 0.700, P > 0.05; ketamine: $F_{1,12}$ = 0.096, P > 0.05). Next, the colocalization of p-GluN2B with PSD95 was examined. In the CA1, CA3 and DG of hippocampus, no significant difference in the colocalization of p-GluN2B and PSD95 was observed in the four groups (Fig. 4g; CA1: interaction: LPS × ketamine, $F_{1,20}$ = 0.773, P > 0.05; LPS: $F_{1,20}$ = 0.057, P > 0.05; ketamine: $F_{1,20}$ = 0.313, P > 0.05; CA3: interaction: LPS × ketamine, $F_{1,20}$ = 2.381, P > 0.05; LPS: $F_{1,20}$ = 0.000, P > 0.05; ketamine: $F_{1,20}$ = 0.381, P > 0.05; DG: interaction: LPS × ketamine, $F_{1,20}$ = 0.356, P > 0.05; LPS: $F_{1,20}$ = 0.181, P > 0.05; ketamine: $F_{1,20}$ = 0.007, P > 0.05). In the CA1 and DG of hippocampus, ketamine treatment reversed the LPS-induced increase in the expression of p-GluN2B (Fig. 4h; CA1: interaction: LPS × ketamine, $F_{1,12}$ = 21.120, P < 0.05; LPS: $F_{1,12}$ = 12.588, P < 0.01; ketamine: $F_{1,12}$ = 11.595, P < 0.01; DG: interaction: LPS × ketamine, $F_{1,12}$ = 15.625, P < 0.05; LPS: $F_{1,12}$ = 52.299, P < 0.01; ketamine: $F_{1,20}$ = 10.632, P < 0.01). This result also suggests that the ketamine-induced reduction in p-GluN2B mainly affects extrasynaptic sites. In summary, these results indicate that the downregulation of GluN2B and p-GluN2B induced by ketamine is mainly derived from the extrasynaptic fractions of the hippocampus.

Ketamine reversed the LPS-induced enhancement of the extrasynaptic interaction of p-CaMKIIα–GluN2B in the hippocampus

Here, a GluN2B antibo dy was used to precipitate the NMDA receptor complex from the extrasynaptic fractions of the hippocampus. Immunoprecipitation assays revealed that p-CaMKIIα binds GluN2B receptors in the extrasynaptic fractions of the hippocampus (Fig. 5a). In addition, ketamine administration attenuated the enhancement of the interaction between p-CaMKIIα (interaction: LPS × ketamine, $F_{1,12}$ = 8.372, P < 0.05; LPS: $F_{1,12}$ =8.207, P < 0.05; ketamine: $F_{1,12}$ =16.954, P < 0.01) and GluN2B (interaction: LPS × ketamine, $F_{1,12}$ =3.117, P > 0.05; LPS: $F1_{,12}$ = 5.341, P < 0.05; ketamine: F1,12 = 9.571, P < 0.01) induced by LPS (Fig. 5b, c). Based on the above results, we hypothesized that the activation of CaMKIIα would affect the extrasynaptic localization and phosphorylation of GluN2B.

Inhibition of CaMKIIα by KN93 prevents depression-like behaviors and reduces elevated extrasynaptic GluN2B localization and phosphorylation in the hippocampus induced by LPS

To determine the relationship between the activation of CaMKIIα and GluN2B, an inhibitor of CaMKIIα, KN93, was used in the present study. Similar to ketamine treatment, KN93 treatment prevented the LPS-induced increase in feeding latency (interaction: LPS × KN93, $F_{1,24} = 30.107$, $P < 0.01$; LPS: $F_{1,24} = 33.146$, $P < 0.01$; KN93: $F_{1,24} = 21.992$, $P < 0.01$; LPS is LPS + DMSO versus Sal + DMSO; KN93 is LPS + KN93 versus LPS + DMSO) in the NSFT, however, no significant difference in the total amount of food consumed was observed in the four groups (Fig. 6a; interaction: LPS × KN93, $F_{1,24} = 0.255$, $P > 0.05$; LPS: $F_{1,24} = 0.954$, $P > 0.05$; KN93: $F_{1,24} = 0.085$, $P > 0.05$). Moreover, in the FST, LPS increased the immobility time, which prevented by KN93 treatment (Fig. 6b; interaction: LPS × KN93, F1,24 = 22.909, $P < 0.01$; LPS: F1,24 = 13.584, $P < 0.01$; KN93: F1,24 = 5.873, $P < 0.05$). These behavioral results suggest that the inhibition of CaMKIIα by KN93 results in an antidepressant phenotype. Furthermore, in the extrasynaptic fractions of hippocampus, KN93 treatment prevented the increase in p-CaMKIIα levels induced by LPS (Fig. 6c; interaction: LPS × KN93, $F_{1,22} = 5.312$, $P < 0.05$; LPS: $F_{1,22} = 4.039$, $P < 0.05$; KN93: $F_{1,22} = 15.795$, $P < 0.01$). Consistent with the assumption that the activation of CaMKIIα affects extrasynaptic GluN2B localization and phosphorylation, LPS increased the level of GluN2B in the extrasynaptic fractions, and this effect was reversed by KN93 treatment (Fig. 6d; interaction: LPS × KN93, $F_{1,25} = 22.571$, $P < 0.05$; LPS: $F_{1,25} = 6.001$, $P < 0.05$; KN93: $F_{1,25} = 8.058$, $P < 0.01$). However, in the synaptic fractions, no significant difference in the level of GluN2B was observed in the four groups (Fig. 6d; interaction: LPS × KN93, $F_{1,12} = 0.002$, $P > 0.05$; LPS: $F_{1,12} = 3.494$, $P > 0.05$; KN93: $F_{1,12} = 0.428$, $P > 0.05$). Next, the colocalization of GluN2B and PSD95 was examined. In the CA1, CA3 and DG of hippocampus, no significant difference in the colocalization of GluN2B and PSD95 was detected in the four groups (Fig. 6h; CA1: interaction: LPS × KN93, $F_{1,20} = 3.375$, $P > 0.05$; LPS: $F_{1,20} = 1.042$, $P > 0.05$; KN93: $F_{1,20} = 0.042$, $P > 0.05$; CA3: interaction: LPS × KN93, $F_{1,20} = 0.632$, $P > 0.05$; LPS: $F_{1,20} = 0.632$, $P > 0.05$; KN93: $F_{1,20} = 0.040$, $P > 0.05$; DG: interaction: LPS × KN93, $F_{1,20} = 0.000$, $P > 0.05$; LPS: $F_{1,20} = 0.032$, $P > 0.05$; KN93: $F_{1,20} = 0.289$, $P > 0.05$). In the CA1, CA3 and DG of hippocampus, KN93 administration reversed the LPS-induced increased in the expression of GluN2B (Fig. 6i; CA1: interaction: LPS × KN93, $F_{1,12} = 21.889$, $P < 0.05$; LPS: $F_{1,12} = 12.144$, $P < 0.01$; KN93: $F_{1,20} = 15.884$, $P < 0.01$; CA3: interaction: LPS × KN93, $F_{1,12} = 8.833$, $P < 0.05$; LPS: $F_{1,12} = 13.404$, $P < 0.01$; KN93: $F_{1,20} = 16.046$, $P < 0.01$; DG: interaction: LPS × KN93, $F_{1,12} = 8.870$, $P < 0.05$; LPS: $F_{1,12} = 18.344$, $P < 0.01$; KN93: $F_{1,20} = 13.806$, $P < 0.01$). This result suggests that the KN93-mediated reduction in GluN2B mainly affects extrasynaptic sites. Furthermore, LPS increased the level of p-GluN2B (S1303) in the extrasynaptic fractions, and this effect was reversed by KN93 treatment (Fig. 6e; interaction: LPS × KN93, $F_{1.12} = 9.784$, $P < 0.05$; LPS: $F_{1,12} = 5.871$, $P < 0.05$; KN93: $F_{1,12} = 18.922$, $P < 0.01$). However, in the synaptic fractions, no significant difference in the level of p-GluN2B was detected in the four groups (Fig. 6e; interaction: LPS × KN93, $F_{1,12} = 0.194$, $P > 0.05$; LPS: $F_{1,12} = 1.157$, $P > 0.05$; KN93: $F_{1,12} = 0.258$, $P > 0.05$). Next, the colocalization of p-GluN2B and PSD95 was examined. In the CA1, CA3 and DG of hippocampus, no significant difference in the colocalization of p-GluN2B and PSD95 was detected in the four groups (Fig. 6j; CA1: interaction: LPS × KN93, $F_{1,20} = 0.169$, $P > 0.05$; LPS: $F_{1,20} = 0.169$, $P > 0.05$; KN93: $F_{1,20} = 0.061$, $P > 0.05$; CA3: interaction: LPS × KN93, $F_{1,20} = 2.609$, $P > 0.05$; LPS: $F_{1,20} = 0.290$, $P > 0.05$; KN93: $F_{1,20} = 0.290$, $P > 0.05$; DG: interaction: LPS × KN93, $F_{1,20} = 0.016$, $P > 0.05$;

LPS: $F_{1,20}$ = 0.16, P > 0.05; KN93: $F_{1,20}$ = 0.016, P > 0.05). In the CA1 and DG of hippocampus, KN93 administration reversed the LPS-induced increased in the level of p-GluN2B (Fig. 6k; CA1: interaction: LPS × KN93, $F_{1,12}$ = 3.688, P < 0.05; LPS: $F_{1,12}$ = 5.904, P < 0.05; KN93: $F_{1,20}$ = 6.328, P < 0.05; DG: interaction: LPS × KN93, $F_{1,12}$ = 24.451, P < 0.05; LPS: $F_{1,12}$ = 29.510, P < 0.01; KN93: $F_{1,20}$ = 12.616, P < 0.01). This result suggests that the KN93-induced reduction in p-GluN2B mainly affects extrasynaptic sites. In summary, the above results indicate that the activity of CaMKIIα is a pivotal part of rapid antidepressant and that the activation of CaMKIIα has an effect on the localization and phosphorylation of GluN2B.

Ketamine up-regulates the expression of p-CREB and BDNF and improves the synaptic dysfunction in the hippocampus

Ketamine administration blocked the LPS-induced significantly decreased in the level of p-CREB in the hippocampus (Fig. 7a; interaction: LPS × ketamine, $F_{1,12}$ =25.310, P < 0.05; LPS: $F_{1,12}$ = 7.936, P < 0.05; ketamine: $F_{1,12}$ = 6.672, P < 0.05). Ketamine administration blocked the LPS-induced significantly decreased in the expression of BDNF in the hippocampus (Fig. 7b; interaction: LPS × ketamine, $F_{1,12}$ = 22.039, P < 0.05; LPS: F1,12 = 6.525, P < 0.05; ketamine: $F_{1,12}$ = 16.408, P < 0.01). Figure 7c shows the time course of the fEPSP data normalized to the level of the 10-min baseline interval. Data from the last 10 min of the post-HFS interval indicated that ketamine sufficiently prevented the LPS-induced depression in SC-CA1 LTP of hippocampus (interaction: LPS × ketamine, $F_{1,8}$ = 10.706, P < 0.05; LPS: $F_{1,8}$ = 7.476, P < 0.05; ketamine: $F_{1,8}$ = 6.972, P < 0.05). Then, the levels of several synaptic proteins in the hippocampal synaptosomes were also analyzed. Ketamine treatment reversed the decrease in GluR1 levels caused by LPS, but did not affect GluR2 levels. (Fig. 7d, e; GluR1: interaction: LPS × ketamine, $F_{1,12}$ = 21.165, P < 0.05; LPS: $F_{1,12}$ = 4.478, P < 0.05; ketamine: $F_{1,12}$ = 9.843, P < 0.01; GluR2: interaction: LPS × ketamine, $F_{1,12}$ = 0.019, P > 0.05; LPS: $F_{1,12}$ = 1.425, P > 0.05; ketamine: $F_{1,12}$ = 0.010, P > 0.05).

Discussion

The results indicate that the decrease in extrasynaptic CaMKIIα activity and the resulting changes in GluN2B localization and phosphorylation were associated with the antidepressant effects of ketamine. Moreover, KN93, a CaMKIIα inhibitor, reduced extrasynaptic GluN2B localization and phosphorylation in the hippocampus, accompanied by the attenuation of depressive-like behaviors. In addition, in the hippocampus, ketamine administration upregulated the expressions of p-CREB and BDNF and prevented the impairment of LTP induction as well as the synaptic protein loss induced by LPS. Therefore, the above results indicate that extrasynaptic CaMKIIα play a pivotal role in the ketamine's antidepressant effects by affecting GluN2B localization and phosphorylation, thereby affecting synaptic plasticity. Here, we propose a model describing a possible pathway for extrasynaptic CaMKIIα to participate in the antidepressant mechanism of ketamine (see Fig. 8).

The LPS-induced depression model induces depression-like behaviors in mice by intraperitoneal injection of LPS. The doses of LPS used in different laboratories are slightly different. It has been reported that LPS at a dose of 0.83 mg/kg can successfully induce depression-like behaviors in mice 24 hours after intraperitoneal injection. In our experiments, we used a dose of 1 mg/kg LPS by dose exploration and verification of depression-related behaviors [27, 33, 34]. Here, in this experiment, depression-like behaviors was successfully induced 24 hours after intraperitoneal injection of 1 mg/kg LPS, and ketamine reversed this depression-like behaviors. In addition, we also found that LPS injection caused anxiety behaviors (in the OFT, the residence time and number of entrances in the central area are reduced), these behaviors could also be blocked by ketamine administration. In support of these results, there is evidence that treatment with ketamine can reduce anxiety-like behavior in animals [35, 36]. In addition, there are still problems that need further explanation. LPS can simultaneously induce acute debilitating symptoms (manifested as acute changes in body weight) and depression-like behaviors [26, 27]. In the present study, LPS decreased body weight, while ketamine did not alter body weight, suggesting that ketamine did not affect LPS-induced acute debilitating symptoms (data not shown). In summary, LPS-induced depression-like behaviors is based on the development of LPS-induced acute debilitating symptoms, but the mechanisms of depression-like behaviors can be separated from the mechanisms of LPS-induced acute debilitating symptoms. LPS-induced acute debilitating symptoms peaks at 4–8 h after injection, while LPS-induced depression-like behaviors present a clear peak at 24 h after injection [37]. Similarly, our results suggest that LPS-induced acute debilitating symptoms is independent of LPS-induced depression-like behaviors, which occur primarily 24 hours after LPS injection.

Many studies have shown that CaMKIIα is involved in the development of depression and pain [38–40]. Clinically relevant studies have shown that the level of CaMKIIα was significantly reduced in the hippocampus of suicidal patients with depression [41]. Another study reported that the mRNA level of CaMKIIα was significantly reduced in the brains of patients with bipolar depression [42]. However, preclinical studies have shown that the inhibition of CaMKIIα improved stress-induced depression-like behaviors [9, 10]. Meanwhile, studies have observed in animal experiments that overexpression of CaMKIIα can block the antidepressant effects of classical antidepressants. After intraperitoneal injection of TATCN21, an inhibitor of CaMKIIα, mice exhibited significant antidepressant behavior in two classic depression-related behavioral tests (the FST and tail suspension test), showing an antidepressant phenotype [40]. Similarly, in the present study, ketamine administration reversed extrasynaptic CaMKIIα activity in the hippocampus. In addition, a CaMKIIα inhibitor, KN93, reversed CaMKIIα activation and attenuated depression-like behaviors. However, preclinical studies have shown that the inhibition of CaMKIIα produces an antidepressant phenotype, which is not consistent with clinical studies. The explanation for this inconsistency are two-fold: First, depression is a complex mental illness involving interactions between the environment and the molecules in the brain, and antidepressants are more likely to induce changes in these molecular mechanisms. Second, the change in CaMKIIα in the brain of patients who die of depression is a terminal phenomenon of the disease. As a typical rapid antidepressant, the changes caused by ketamine may be more of an initial phenomenon. There may be some differences between the two. In addition, it should be mentioned that, in general, the physiological

function of CaMKIIα is considered to be important for the formation and maintenance of dendrites, which are the structural basis for synaptic plasticity [24, 43]. However, how does the inhibition of CaMKIIα activity in the hippocampus lead to behavioral effects similar to those of antidepressants? A premature speculation is that large increases or decreases in synaptic plasticity are unfavorable, and that inhibiting CaMKIIα may reverse large increases in synaptic plasticity.

CaMKII can participate in the regulation of numerous physiological processes by interacting with a variety of substrate molecules [8]. It has been reported that CaMKII can stay at the postsynaptic site for a longer time by binding to GluN2B, and this interaction is considered to be crucial for synaptic structure and strength [44, 45]. The study on CaMKII and GluN2B mainly focuses on the post-synapse and relatively few extrasynapses It should be mentioned that the location of the protein is different, and its role in participating in physiological and pathological processes is also different [46–48]. Here, ketamine administration reversed extrasynaptic CaMKIIα activity and reduced extrasynaptic GluN2B localization and phosphorylation in the hippocampus. The difference is that ketamine does not affect the activity of postsynaptic CaMKIIα and the localization and phosphorylation of GluN2B. A premature speculation is that ketamine tends to inhibit GluN2B-containing NMDA receptors, which are mainly locate in the eatrasynapse. In addition, p-CaMKIIα binding to GluN2B and ketamine administration attenuated the enhanced interaction between p-CaMKIIα and GluN2B. Similarly, studies have shown that in a model of LPS-induced neuronal injury, GluN2B antagonists can reverse neuronal damage by disrupting a signaling complex such as GluN2B–CaMKII–PSD95 and further reducing the level of phosphorylated CaMKII [49]. In general, Ca^{2+} can flow into the cell through the GluN2B-containing NMDA receptors on the membrane, causing phosphorylation of CaMKIIα at the Thr286 site. Subsequently, activated CaMKIIα can phosphorylate the GluN2B receptor, further promoting Ca^{2+} influx into the cell. Therefore, CaMKIIα and the GluN2B receptor may interact in a positive feedback manner. In the present study, the inhibition of CaMKIIα activity by KN93 reduced extrasynaptic GluN2B localization and phosphorylation in the hippocampus. This further complements the previous hypothesis that ketamine preferentially inhibits extrasynaptic GluN2B [13], this data show that CaMKIIα is also involved in the antidepressant effect of ketamine, and its downstream also involves GluN2B, which may help broaden our understanding of rapid antidepression.

A certain degree of NMDARs activity is crucial to neurotransmission [50]. Excessively enhanced NMDARs activity can lead to intracellular calcium overload and trigger a series of pathological processes, including depression [51, 52]. The specific effects of NMDARs activation depend mainly on the subcellular localization of the receptor [53]. Synaptic NMDAR activation promotes CREB phosphorylation, whereas extrasynaptic NMDAR activation decreases CREB phosphorylation [11, 54]. Furthermore, the BDNF gene is controlled by several transcription factors, and CREB plays a central role in this regulatory process [55, 56]. Antidepressants can increase BDNF levels in the hippocampus, while viral knockout of BNDF in specific subregions of the hippocampus can induce depression-like behaviors [57]. Here, LPS injection decreased the levels of p-CREB and BDNF in the hippocampus, which reversed by ketamine treatment. In support of our results, the GluN2B antagonist was shown to rapidly reverse depression-like behaviors and

normalize the levels of p-CREB and BDNF in the medial prefrontal cortex. These results illustrate that the CREB inhibition pathway induced by overactivated extrasynaptic GluN2B participated in ketamine's antidepressant effects.

The disruption of synaptic plasticity is considered to be one of the neurobiological manifestations of depression [25], and AMPA receptors occupies a critical position in the formation, maintenance, and homeostasis of synaptic plasticity [58]. Studies have shown that AMPARs can be quickly transported to synapses during LTP [59, 60]. Adult knockout mice lacking GluR1 do not show LTP, suggesting that the GluR1 subunit is essential for the production of LTP. It has been reported that the classic antidepressant fluoxetine can enhance the LTP of the hippocampus [61]. AMPAR subunits (GluR1 and GluR2) were upregulated in the hippocampus after ketamine administration [28]. Pretreatment with the AMPAR antagonist NBQX was observed to block the antidepressant effects of ketamine in a variety of animal models of depression [15, 62]. In this study, ketamine prevented the impaired LTP induction induced by LPS. Moreover, ketamine significantly increased the level of the GluR1 subunit but did not alter the level of the GluR2 subunit in the hippocampal synaptosomes. This data show that the core of rapid antidepressant effects of ketamine shifts from early functional plasticity to late structural homeostasis [63].

There are some limitations to our study. First, due to the limitations of acute experiments, we did not continue to observe changes in CaMKIIα over a longer period of time after ketamine administration. Therefore, the late effects of CaMKIIα after ketamine administration are for further study. Second, clinical and basic studies have shown that the antidepressant effects of ketamine produce different results in different gender situations [64, 65]. Notably, the incidence of major depression in women is approximately twice that in men [66, 67]. Therefore, further study on gender differences is needed. Third, we did not overexpress CaMKIIα to verify whether overexpression can block ketamine's antidepressant effects due to the particularity and precision of the extrasynaptic fraction. In the future, the different effects of ketamine on CaMKIIα (extrasynaptic fraction and synaptic fraction) may be further observed in primary neuron culture. At the same time, the results suggest that the responses to stimulation and treatment differ in extrasynaptic and synaptic fraction.

Conclusion

In conclusion, our results indicate that ketamine is effective in reversing LPS-induced depression-like behaviors, a process associated with decreased extrasynaptic CaMKIIα activity in the hippocampus. The downstream events induced by CaMKIIα include the regulation of extrasynaptic GluN2B localization and phosphorylation, which subsequently affected synaptic plasticity. A more detailed understanding of the antidepressant mechanism of ketamine will help us find the target of rapid antidepressant, which will contribute to the development of the next generation of more effective and safer antidepressants.

Abbreviations

CaMKII:Calcium/calmodulin-dependent protein kinase II; NMDARs:N-methyl-D-aspartate receptors; LPS:Lipopolysaccharide; PSD95:Postsynaptic density-95; BCA:Bicinchoninic acid; ACSF:Artificial cerebrospinal fluid; HFS:High-frequency stimulation; fEPSP:Field excitatory postsynaptic potential; OFT:Open field test; NSFT:Novelty-suppressed feeding test; FST:Forced swimming test; KN-93:C26H29ClN2O4S.H3O4P; DMSO:Dimethyl sulfoxide

Declarations

Acknowledgments

The authors would like to thank the MARC of Nanjing University and the staff for providing animal care during this study.

Authors' contributions

XHT and GFZ designed this work. XHT wrote the paper. XHT, NX and RL performed the experiments. XHT, MJ and GFD analyzed the data. ZQZ and JJY directed the discussion. All authors read and approved the final manuscript.

Funding

This study was supported by grants from the National Natural Science Foundation of China (to G.F.Z., No.81503053, and Z.Q.Z., No.81571083).

Availability of data and materials

The data that support the findings of this study are available from the corresponding author upon reasonable request.

Ethics approval and consent to participate

All animal experiments and related operations are carried out in accordance with the Guideline for the Care and Use of Laboratory Animals from Model Animal Research Center (MARC) of Nanjing University and the National Institutes of Health.

Consent for publication

Not applicable

Competing interests

The authors declare that they have no competing interests.

Author details

[1]Department of Anesthesiology, Zhongda Hospital, School of Medicine, Southeast University, Nanjing, Jiangsu, China. [2]Minister of Education Key Laboratory of Model Animal for Disease Study, Model Animal Research Center, Nanjing University, Nanjing, Jiangsu, China. [3]Department of Anesthesiology, Jinling Hospital, School of Medicine, Nanjing University, Nanjing, Jiangsu, China. [4]Department of Anesthesiology, Pain and Perioperative Medicine, The First Affiliated Hospital of Zhengzhou University, Zhengzhou, Henan, China

References

1. Kessler RC, Berglund P, Demler O, Jin R, Koretz D, Merikangas KR et al. The epidemiology of major depressive disorder: results from the National Comorbidity Survey Replication (NCS-R). JAMA. 2003; 289:3095-3105.
2. Insel TR, Wang PS. The STAR*D trial: revealing the need for better treatments. Psychiatr Serv. 2009; 60:1466-1467.
3. Berman RM, Cappiello A, Anand A, Oren DA, Heninger GR, Charney DS et al. Antidepressant effects of ketamine in depressed patients. Biol Psychiatry. 2000; 47:351-354.
4. Diazgranados N, Ibrahim L, Brutsche NE, Newberg A, Kronstein P, Khalife S et al. A randomized add-on trial of an N-methyl-D-aspartate antagonist in treatment-resistant bipolar depression. Arch Gen Psychiatry. 2010; 67:793-802.
5. Price RB, Nock MK, Charney DS, Mathew SJ. Effects of intravenous ketamine on explicit and implicit measures of suicidality in treatment-resistant depression. Biol Psychiatry. 2009; 66:522-526.
6. Hudmon A, Schulman H. Neuronal CA2+/calmodulin-dependent protein kinase II: the role of structure and autoregulation in cellular function. Annu Rev Biochem. 2002; 71:473-510.
7. Wayman GA, Lee YS, Tokumitsu H, Silva AJ, Soderling TR. Calmodulin-kinases: modulators of neuronal development and plasticity. Neuron. 2008; 59:914-931.
8. Lisman J, Schulman H, Cline H. The molecular basis of CaMKII function in synaptic and behavioural memory. Nat Rev Neurosci. 2002; 3:175-190.
9. Kim TK, Kim JE, Park JY, Lee JE, Choi J, Kim H et al. Antidepressant effects of exercise are produced via suppression of hypocretin/orexin and melanin-concentrating hormone in the basolateral amygdala. Neurobiol Dis. 2015; 79:59-69.
10. Robison AJ, Vialou V, Sun HS, Labonte B, Golden SA, Dias C et al. Fluoxetine epigenetically alters the CaMKIIalpha promoter in nucleus accumbens to regulate DeltaFosB binding and antidepressant effects. Neuropsychopharmacology. 2014; 39:1178-1186.
11. Hardingham GE, Bading H. Synaptic versus extrasynaptic NMDA receptor signalling: implications for neurodegenerative disorders. Nat Rev Neurosci. 2010; 11:682-696.
12. Vyklicky V, Korinek M, Smejkalova T, Balik A, Krausova B, Kaniakova M et al. Structure, function, and pharmacology of NMDA receptor channels. Physiol Res. 2014; 63 Suppl 1:S191-203.

13. Miller OH, Yang L, Wang CC, Hargroder EA, Zhang Y, Delpire E et al. GluN2B-containing NMDA receptors regulate depression-like behavior and are critical for the rapid antidepressant actions of ketamine. eLife. 2014; 3:e03581.
14. Kiselycznyk C, Jury NJ, Halladay LR, Nakazawa K, Mishina M, Sprengel R et al. NMDA receptor subunits and associated signaling molecules mediating antidepressant-related effects of NMDA-GluN2B antagonism. Behav Brain Res. 2015; 287:89-95.
15. Maeng S, Zarate CA, Jr., Du J, Schloesser RJ, McCammon J, Chen G et al. Cellular mechanisms underlying the antidepressant effects of ketamine: role of alpha-amino-3-hydroxy-5-methylisoxazole-4-propionic acid receptors. Biol Psychiatry. 2008; 63:349-352.
16. Wang CC, Held RG, Chang SC, Yang L, Delpire E, Ghosh A et al. A critical role for GluN2B-containing NMDA receptors in cortical development and function. Neuron. 2011; 72:789-805.
17. Ibrahim L, Diaz Granados N, Jolkovsky L, Brutsche N, Luckenbaugh DA, Herring WJ et al. A Randomized, placebo-controlled, crossover pilot trial of the oral selective NR2B antagonist MK-0657 in patients with treatment-resistant major depressive disorder. J Clin Psychopharmacol. 2012; 32:551-557.
18. Tavalin SJ, Colbran RJ. CaMKII-mediated phosphorylation of GluN2B regulates recombinant NMDA receptor currents in a chloride-dependent manner. Mol Cell Neurosci. 2017; 79:45-52.
19. Bayer KU, De Koninck P, Leonard AS, Hell JW, Schulman H. Interaction with the NMDA receptor locks CaMKII in an active conformation. Nature. 2001; 411:801-805.
20. Barcomb K, Hell JW, Benke TA, Bayer KU. The CaMKII/GluN2B Protein Interaction Maintains Synaptic Strength. J Biol Chem. 2016; 291:16082-16089.
21. Shonesy BC, Jalan-Sakrikar N, Cavener VS, Colbran RJ. CaMKII: a molecular substrate for synaptic plasticity and memory. Prog Mol Biol Transl Sci. 2014; 122:61-87.
22. Hell JW. CaMKII: claiming center stage in postsynaptic function and organization. Neuron. 2014; 81:249-265.
23. Coultrap SJ, Bayer KU. CaMKII regulation in information processing and storage. Trends Neurosci. 2012; 35:607-618.
24. Colbran RJ. Targeting of calcium/calmodulin-dependent protein kinase II. Biochem J. 2004; 378:1-16.
25. Duman RS, Aghajanian GK. Synaptic dysfunction in depression: potential therapeutic targets. Science. 2012; 338:68-72.
26. Walker AK, Budac DP, Bisulco S, Lee AW, Smith RA, Beenders B et al. NMDA receptor blockade by ketamine abrogates lipopolysaccharide-induced depressive-like behavior in C57BL/6J mice. Neuropsychopharmacology. 2013; 38:1609-1616.
27. O'Connor JC, Lawson MA, Andre C, Moreau M, Lestage J, Castanon N et al. Lipopolysaccharide-induced depressive-like behavior is mediated by indoleamine 2,3-dioxygenase activation in mice. Mol Psychiatry. 2009; 14:511-522.

28. Zanos P, Moaddel R, Morris PJ, Georgiou P, Fischell J, Elmer GI et al. NMDAR inhibition-independent antidepressant actions of ketamine metabolites. Nature. 2016; 533:481-486.
29. Yang Y, Cui Y, Sang K, Dong Y, Ni Z, Ma S et al. Ketamine blocks bursting in the lateral habenula to rapidly relieve depression. Nature. 2018; 554:317-322.
30. Li S, Jin M, Koeglsperger T, Shepardson NE, Shankar GM, Selkoe DJ. Soluble Abeta oligomers inhibit long-term potentiation through a mechanism involving excessive activation of extrasynaptic NR2B-containing NMDA receptors. J Neurosci. 2011; 31:6627-6638.
31. Li N, Lee B, Liu RJ, Banasr M, Dwyer JM, Iwata M et al. mTOR-dependent synapse formation underlies the rapid antidepressant effects of NMDA antagonists. Science. 2010; 329:959-964.
32. Li SX, Han Y, Xu LZ, Yuan K, Zhang RX, Sun CY et al. Uncoupling DAPK1 from NMDA receptor GluN2B subunit exerts rapid antidepressant-like effects. Mol Psychiatry. 2018; 23:597-608.
33. Tang MM, Lin WJ, Zhang JT, Zhao YW, Li YC. Exogenous FGF2 reverses depressive-like behaviors and restores the suppressed FGF2-ERK1/2 signaling and the impaired hippocampal neurogenesis induced by neuroinflammation. Brain Behav Immun. 2017; 66:322-331.
34. Brooks AK, Janda TM, Lawson MA, Rytych JL, Smith RA, Ocampo-Solis C et al. Desipramine decreases expression of human and murine indoleamine-2,3-dioxygenases. Brain Behav Immun. 2017; 62:219-229.
35. Jiang Y, Wang Y, Sun X, Lian B, Sun H, Wang G et al. Short- and long-term antidepressant effects of ketamine in a rat chronic unpredictable stress model. Brain Behav. 2017; 7:e00749.
36. Holubova K, Kleteckova L, Skurlova M, Ricny J, Stuchlik A, Vales K. Rapamycin blocks the antidepressant effect of ketamine in task-dependent manner. Psychopharmacology (Berl). 2016; 233:2077-2097.
37. Frenois F, Moreau M, O'Connor J, Lawson M, Micon C, Lestage J et al. Lipopolysaccharide induces delayed FosB/DeltaFosB immunostaining within the mouse extended amygdala, hippocampus and hypothalamus, that parallel the expression of depressive-like behavior. Psychoneuroendocrinology. 2007; 32:516-531.
38. Hu X, Huang F, Wang ZJ. CaMKIIalpha Mediates the Effect of IL-17 To Promote Ongoing Spontaneous and Evoked Pain in Multiple Sclerosis. J Neurosci. 2018; 38:232-244.
39. Chen Y, Yang C, Wang ZJ. Ca2+/calmodulin-dependent protein kinase II alpha is required for the initiation and maintenance of opioid-induced hyperalgesia. J Neurosci. 2010; 30:38-46.
40. Adaikkan C, Taha E, Barrera I, David O, Rosenblum K. Calcium/Calmodulin-Dependent Protein Kinase II and Eukaryotic Elongation Factor 2 Kinase Pathways Mediate the Antidepressant Action of Ketamine. Biol Psychiatry. 2018; 84:65-75.
41. Fuchsova B, Alvarez Julia A, Rizavi HS, Frasch AC, Pandey GN. Altered expression of neuroplasticity-related genes in the brain of depressed suicides. Neuroscience. 2015; 299:1-17.
42. Xing G, Russell S, Hough C, O'Grady J, Zhang L, Yang S et al. Decreased prefrontal CaMKII alpha mRNA in bipolar illness. Neuroreport. 2002; 13:501-505.

43. Jiang X, Chai GS, Wang ZH, Hu Y, Li XG, Ma ZW et al. CaMKII-dependent dendrite ramification and spine generation promote spatial training-induced memory improvement in a rat model of sporadic Alzheimer's disease. Neurobiol Aging. 2015; 36:867-876.
44. Halt AR, Dallapiazza RF, Zhou Y, Stein IS, Qian H, Juntti S et al. CaMKII binding to GluN2B is critical during memory consolidation. EMBO J. 2012; 31:1203-1216.
45. Martel MA, Ryan TJ, Bell KF, Fowler JH, McMahon A, Al-Mubarak B et al. The subtype of GluN2 C-terminal domain determines the response to excitotoxic insults. Neuron. 2012; 74:543-556.
46. Goebel-Goody SM, Davies KD, Alvestad Linger RM, Freund RK, Browning MD. Phospho-regulation of synaptic and extrasynaptic N-methyl-d-aspartate receptors in adult hippocampal slices. Neuroscience. 2009; 158:1446-1459.
47. Parsons MP, Raymond LA. Extrasynaptic NMDA receptor involvement in central nervous system disorders. Neuron. 2014; 82:279-293.
48. Ivanov A, Pellegrino C, Rama S, Dumalska I, Salyha Y, Ben-Ari Y et al. Opposing role of synaptic and extrasynaptic NMDA receptors in regulation of the extracellular signal-regulated kinases (ERK) activity in cultured rat hippocampal neurons. J Physiol. 2006; 572:789-798.
49. Song Y, Zhao X, Wang D, Zheng Y, Dai C, Guo M et al. Inhibition of LPS-induced brain injury by NR2B antagonists through reducing assembly of NR2B-CaMKII-PSD95 signal module. Immunopharmacol Immunotoxicol. 2019:1-9.
50. Hardingham GE, Bading H. The Yin and Yang of NMDA receptor signalling. Trends Neurosci. 2003; 26:81-89.
51. Arundine M, Tymianski M. Molecular mechanisms of calcium-dependent neurodegeneration in excitotoxicity. Cell Calcium. 2003; 34:325-337.
52. Kim YK, Na KS. Role of glutamate receptors and glial cells in the pathophysiology of treatment-resistant depression. Prog Neuropsychopharmacol Biol Psychiatry. 2016; 70:117-126.
53. Kohr G. NMDA receptor function: subunit composition versus spatial distribution. Cell Tissue Res. 2006; 326:439-446.
54. Hardingham GE, Fukunaga Y, Bading H. Extrasynaptic NMDARs oppose synaptic NMDARs by triggering CREB shut-off and cell death pathways. Nat Neurosci. 2002; 5:405-414.
55. West AE, Chen WG, Dalva MB, Dolmetsch RE, Kornhauser JM, Shaywitz AJ et al. Calcium regulation of neuronal gene expression. Proc Natl Acad Sci U S A. 2001; 98:11024-11031.
56. Vanhoutte P, Bading H. Opposing roles of synaptic and extrasynaptic NMDA receptors in neuronal calcium signalling and BDNF gene regulation. Curr Opin Neurobiol. 2003; 13:366-371.
57. Taliaz D, Stall N, Dar DE, Zangen A. Knockdown of brain-derived neurotrophic factor in specific brain sites precipitates behaviors associated with depression and reduces neurogenesis. Mol Psychiatry. 2010; 15:80-92.
58. Derkach VA, Oh MC, Guire ES, Soderling TR. Regulatory mechanisms of AMPA receptors in synaptic plasticity. Nat Rev Neurosci. 2007; 8:101-113.

59. Penn AC, Zhang CL, Georges F, Royer L, Breillat C, Hosy E et al. Hippocampal LTP and contextual learning require surface diffusion of AMPA receptors. Nature. 2017; 549:384-388.
60. Gu J, Lee CW, Fan Y, Komlos D, Tang X, Sun C et al. ADF/cofilin-mediated actin dynamics regulate AMPA receptor trafficking during synaptic plasticity. Nat Neurosci. 2010; 13:1208-1215.
61. Bath KG, Jing DQ, Dincheva I, Neeb CC, Pattwell SS, Chao MV et al. BDNF Val66Met impairs fluoxetine-induced enhancement of adult hippocampus plasticity. Neuropsychopharmacology. 2012; 37:1297-1304.
62. Fukumoto K, Iijima M, Chaki S. The Antidepressant Effects of an mGlu2/3 Receptor Antagonist and Ketamine Require AMPA Receptor Stimulation in the mPFC and Subsequent Activation of the 5-HT Neurons in the DRN. Neuropsychopharmacology. 2016; 41:1046-1056.
63. Zanos P, Gould TD. Mechanisms of ketamine action as an antidepressant. Mol Psychiatry. 2018; 23:801-811.
64. Marcus SM, Young EA, Kerber KB, Kornstein S, Farabaugh AH, Mitchell J et al. Gender differences in depression: findings from the STAR*D study. J Affect Disord. 2005; 87:141-150.
65. Picard N, Takesian AE, Fagiolini M, Hensch TK. NMDA 2A receptors in parvalbumin cells mediate sex-specific rapid ketamine response on cortical activity. Mol Psychiatry. 2019.
66. Grigoriadis S, Robinson GE. Gender issues in depression. Ann Clin Psychiatry. 2007; 19:247-255.
67. Holden C. Sex and the suffering brain. Science. 2005; 308:1574.

Figures

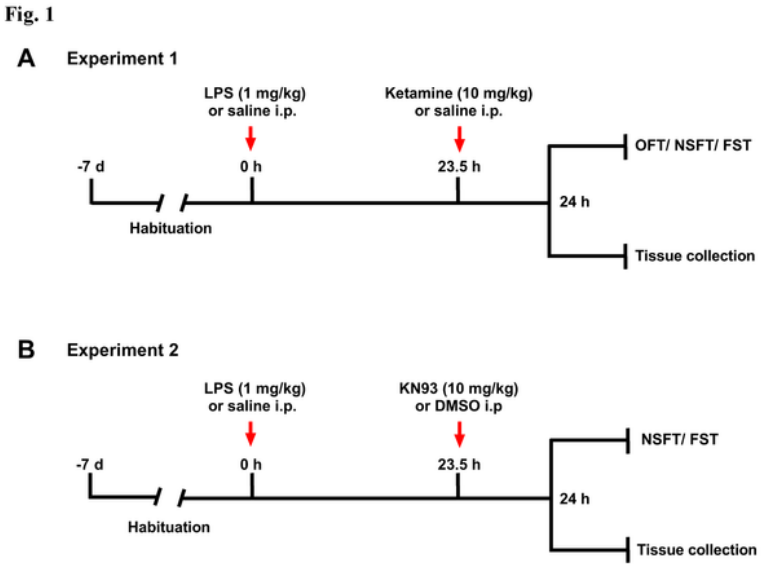

Figure 1

Timeline of drug injection, behavioral testing and tissue collection: experiment 1 a and experiment 2 b. LPS, lipopolysaccharide; OFT, open field test; NSFT, novelty-suppressed feeding test; FST, forced swimming test; KN-93, C26H29ClN2O4S.H3O4P; DMSO, dimethyl sulfoxide

Fig. 2

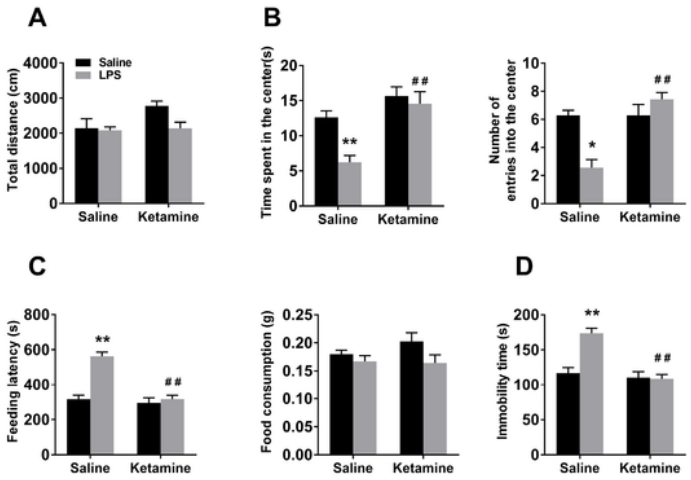

Figure 2

LPS-induced depression-like behaviors were rescued by ketamine treatment. a In OFT, there was no significant difference in the free movement distance between the four groups of mice within 5 minutes. b Ketamine administration prevented the LPS-induced decrease in time spent in the center and the number of entries into the center in the OFT. C In the NSFT, ketamine administration prevented the LPS-induced increase in feeding latency, but the total amount of food consumed in the home cage in a 15-min test

was not different among the four groups. d In the FST, ketamine administration prevented the increase in immobility time induced by LPS. Data are presented as the mean ± SEM (n = 7–10 mice per group). *p < 0.05, **p < 0.01 compared with the Sal + Sal group; ##p < 0.01 compared with the LPS + Sal group. Sal: saline

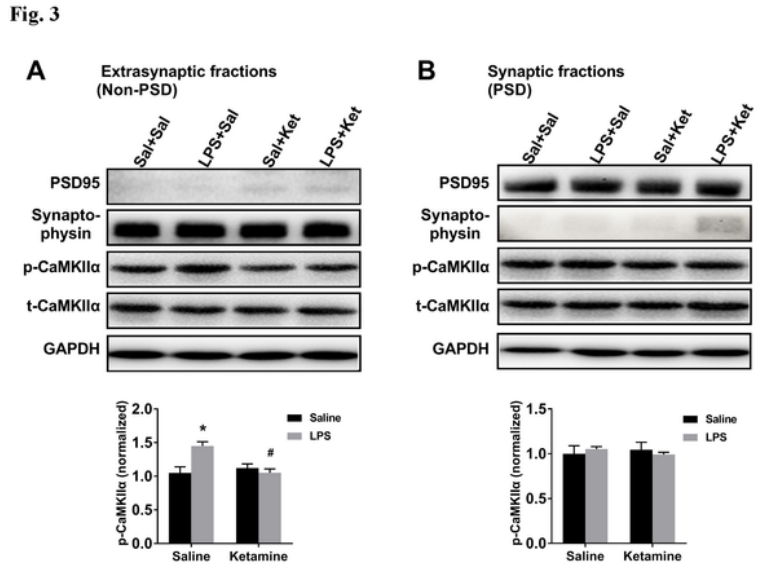

Figure 3

The levels of p-CaMKIIα and CaMKIIα in the extrasynaptic and synaptic fractions of the hippocampus were determined by Western blotting. a In the extrasynaptic fractions of the hippocampus, ketamine administration reversed the elevated level of p-CaMKIIα induced by LPS injection. b In the synaptic fractions of the hippocampus, no significant difference in the level of p-CaMKIIα was observed in the four groups. Data are presented as the mean ± SEM (n = 4–6 mice per group). *p < 0.05 compared with the Sal + Sal group; #p < 0.05 compared with the LPS + Sal group

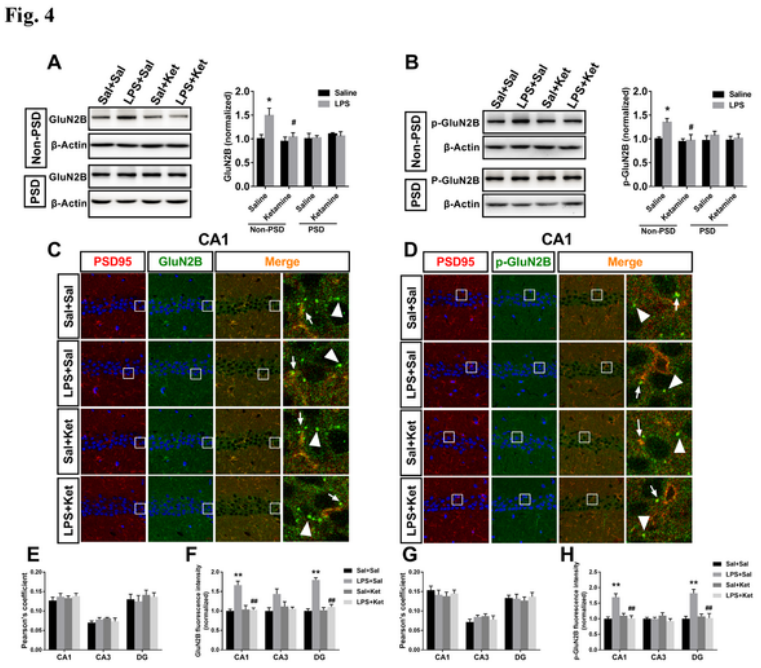

Figure 4

Ketamine decreased the LPS-induced increase in extrasynaptic localization and phosphorylation of GluN2B in the hippocampus. The levels of GluN2B and p-GluN2B in the extrasynaptic and synaptic fractions of the hippocampus were determined by Western blotting. a Ketamine treatment reversed the LPS-induced increase in the level of extrasynaptic GluN2B but did not affect the level of synaptic GluN2B in the hippocampus. b Ketamine treatment reversed the LPS-induced increase in the level of extrasynaptic p-GluN2B but did not affect the level of synaptic p-GluN2B in the hippocampus. c Immunofluorescent images show the colocalization of PSD95 (red) and surface GluN2B receptor (green) in the CA1 regions of the hippocampus. High magnification images of the region are delineated by the white square and shown to the right. The arrow indicates colocalization, and the triangle indicates no colocalization. d Immunofluorescent images show the colocalization of PSD95 (red) and p-GluN2B (green) in the CA1 regions of the hippocampus. High magnification images of the region are delineated by the white square and shown to the right. The arrow indicates colocalization, and the triangle indicates no colocalization. e Pearson's correlation coefficient of PSD95 and GluN2B was not significantly different among the four groups in the CA1, CA3 and DG of the hippocampus. f LPS up-regulated the levels of GluN2B in the CA1 and DG of the hippocampus, and this increase was reversed by ketamine administration. g Pearson's correlation coefficient of PSD95 and p-GluN2B was not significantly different among the four groups in the CA1, CA3 and DG of the hippocampus. h LPS up-regulated the levels of p-GluN2B in the CA1 and DG of the hippocampus, and this effect was reversed by ketamine administration. Scale bars represent 10 μm. Data are presented as the mean ± SEM (n = 4–6 mice per group). *p < 0.05, **p < 0.01 compared with the Sal + Sal group; #p < 0.05, ##p < 0.01 compared with the LPS + Sal group

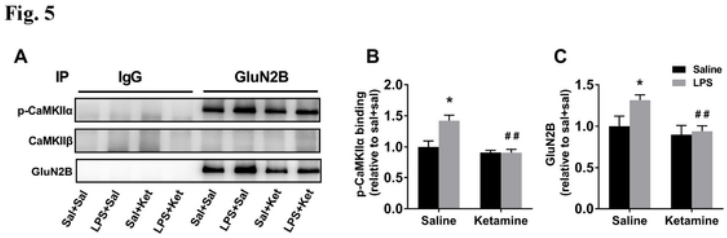

Figure 5

Ketamine decreased the enhanced extrasynaptic p-CaMKIIα–GluN2B interaction in the hippocampus induced by LPS. a Immunoprecipitation of GluN2B with p-CaMKIIα and CaMKIIβ in the extrasynaptic fractions of the hippocampus. b, c Ketamine administration attenuated the enhanced interaction between p-CaMKIIα and GluN2B induced by LPS. Data are presented as the mean ± SEM (n = 4–6 mice per group). *p < 0.05 compared with the Sal + Sal group; ##p < 0.01 compared with the LPS + Sal group

Fig. 6

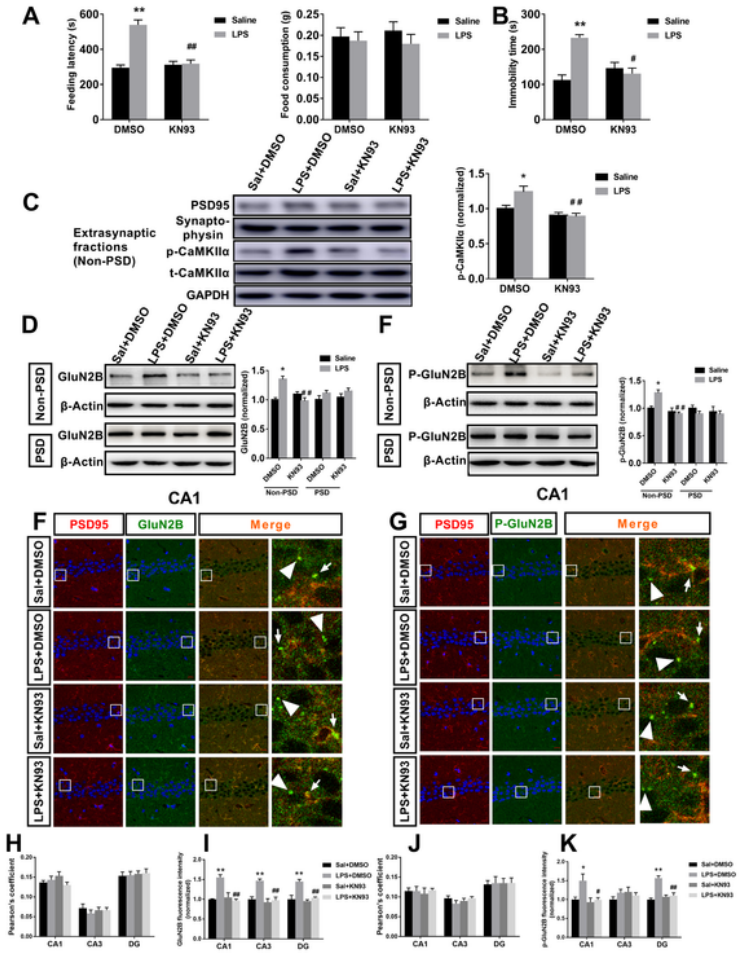

Figure 6

Inhibition of CaMKIIα by KN93 prevents the depression-like behaviors and reduces the elevated extrasynaptic GluN2B localization and phosphorylation in the hippocampus induced by LPS a KN93 administration prevented the LPS-induced increase in feeding latency in the NSFT, but the total amount of food consumed in the home cage in a 15-min test was not different among the four groups. b KN93 administration prevented the increase in immobility time in the FST induced by LPS. c In the

extrasynaptic fractions of the hippocampus, KN93 administration reversed the elevated level of p-CaMKIIα induced by LPS injection. d KN93 treatment reversed the LPS-induced increase in the level of extrasynaptic GluN2B but did not affect the level of synaptic GluN2B in the hippocampus. e KN93 treatment reversed the LPS-induced increase in the level of extrasynaptic p-GluN2B but did not affect the level of synaptic p-GluN2B in the hippocampus. f Immunofluorescent images show the colocalization of PSD95 (red) and surface GluN2B receptor (green) in the CA1 regions of the hippocampus. High magnification images of the region are delineated by the white square and shown to the right. The arrow indicates colocalization, and the triangle indicates no colocalization. g Immunofluorescent images show the colocalization of PSD95 (red) with p-GluN2B (green) in the CA1 regions of the hippocampus. High magnification images of the region are delineated by the white square and shown to the right. The arrow indicates colocalization, and the triangle indicates no colocalization. h Pearson's correlation coefficient of PSD95 and GluN2B was not significantly different among the four groups in the CA1, CA3 and DG of the hippocampus. i LPS up-regulated the levels of GluN2B in the CA1, CA3 and DG of the hippocampus, and this increase was reversed by KN93 administration. j Pearson's correlation coefficient of PSD95 and p-GluN2B was not significantly different among the four groups in the CA1, CA3 and DG of the hippocampus. k LPS up-regulated the levels of p-GluN2B in the CA1 and DG of the hippocampus, and this effect was reversed by KN93 administration. Scale bars indicate 10 μm. Data are presented as the mean ± SEM (n = 4–10 mice per group). *p < 0.05, **p < 0.01 compared with the Sal + DMSO group; #p < 0.05, ##p < 0.01 compared with the LPS + DMSO group

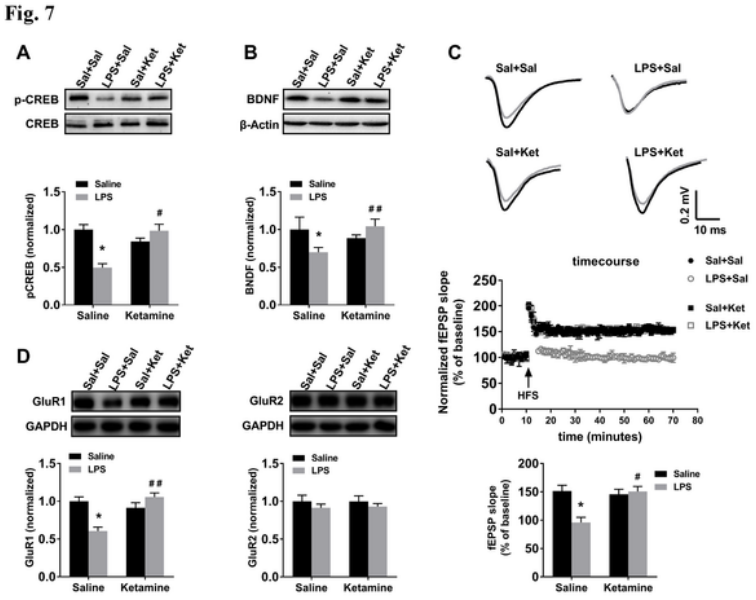

Figure 7

Ketamine rescues the LPS-induced down-regulation of p-CREB and BDNF and the synaptic dysfunction in the hippocampus. a LPS significantly decreased the expression of p-CREB in the hippocampus, and this effect was blocked by ketamine administration. b LPS significantly down-regulated the level of BDNF in the hippocampus, and this decrease was blocked by ketamine administration. c Schematic representation of the four groups of EPSPs recorded before (grey) and after (black) HFS. Horizontal

calibration bars, 10 ms; vertical bars, 0.2 mV. Time course of fEPSP data normalized to the level of the 10-min baseline interval. Ketamine prevented the LPS-induced depression of SC-CA1 LTP in the hippocampus. d, e In hippocampal synaptosomes, ketamine treatment reversed the decrease in GluR1 levels caused by LPS, but did not affect GluR2 levels. Data are presented as the mean ± SEM (n = 4-7 mice per group). *p < 0.05 compared with the Sal + Sal group; #p < 0.05, ##p < 0.01 compared with the LPS + Sal group

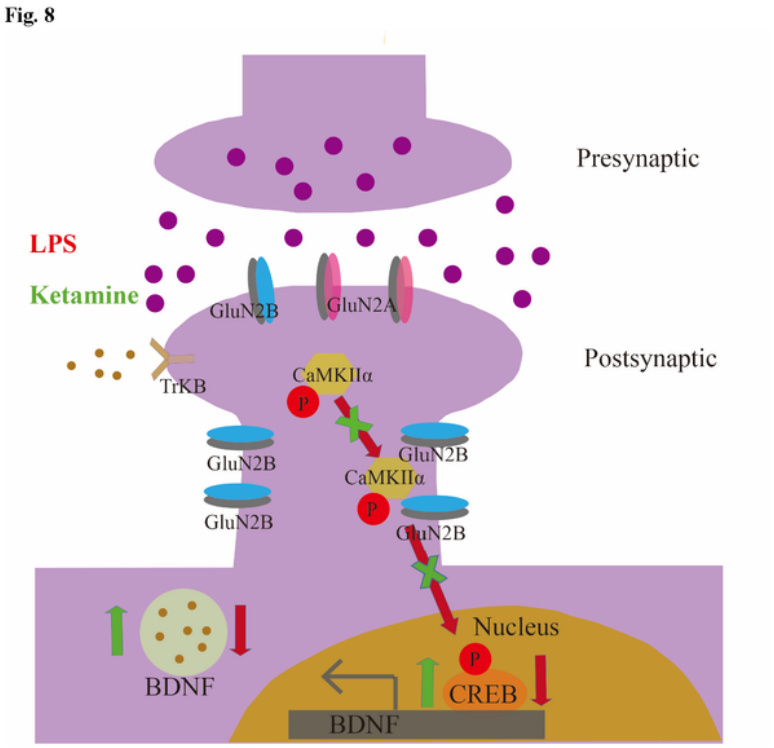

Figure 8

Schematic diagram that illustrates the involvement of CaMKIIα in mediating the localization and phosphorylation of GluN2B in the hippocampus under the treatment with the antidepressant drug ketamine. LPS stimulation induces extrasynaptic CaMKIIα T286 autophosphorylation (p-CaMKIIα) and subsequently induces p-CaMKIIα binding to GluN2B in the extrasynaptic region of the hippocampus, which causes GluN2B retention on the membrane and GluN2B phosphorylation. The activation of GluN2B downregulates p-CREB and BDNF levels and subsequently impairs LTP induction as well as induces synaptic protein deficits in the hippocampus, ultimately leading to depression-like behaviors. Ketamine administration selectively reversed the activation of CaMKIIα in the extrasynaptic hippocampus, followed by the normalization of GluN2B localization and phosphorylation, which increased the levels of p-CREB, BDNF and synaptic proteins in the hippocampus and finally rescued depression-like behaviors